

VU Research Portal

Immune modulation of bone marrow-derived cells in Ischemic Heart Disease

Yildirim, C.

2015

document version

Publisher's PDF, also known as Version of record

[Link to publication in VU Research Portal](#)

citation for published version (APA)

Yildirim, C. (2015). *Immune modulation of bone marrow-derived cells in Ischemic Heart Disease*. [PhD-Thesis - Research and graduation internal, Vrije Universiteit Amsterdam].

General rights

Copyright and moral rights for the publications made accessible in the public portal are retained by the authors and/or other copyright owners and it is a condition of accessing publications that users recognise and abide by the legal requirements associated with these rights.

- Users may download and print one copy of any publication from the public portal for the purpose of private study or research.
- You may not further distribute the material or use it for any profit-making activity or commercial gain
- You may freely distribute the URL identifying the publication in the public portal ?

Take down policy

If you believe that this document breaches copyright please contact us providing details, and we will remove access to the work immediately and investigate your claim.

E-mail address:

vuresearchportal.ub@vu.nl

Chapter 4

Palmitic acid increases pro-oxidant adaptor protein p66Shc expression and affects vascularization factors in angiogenic mononuclear cells: action of resveratrol

Julie Favre¹

Cansu Yildirim¹

Thomas A. Leyen¹

Weena J.Y. Chen²

Renate E. van Genugten²

Larissa W. van Golen²

Juan J. Garcia-Vallejo¹

Rene Musters³

Josefien M. Baggen¹

Ruud D. Fontijn¹

Tineke C.T.M. van der Pouw Kraan¹

Erik Serné²

Pieter Koolwijk³

Michaela Diamant²

Anton J.G. Horrevoets

¹ Department of Molecular Cell Biology and Immunology, VU University Medical Center, Amsterdam, The Netherlands

² Department of Diabetes Center Internal medicine, VU University Medical Center, Amsterdam, The Netherlands

³ Department of Physiology, VU University Medical Center, Amsterdam, The Netherlands

ABSTRACT

A defect in neovascularization process involving circulating angiogenic mononuclear cells (CACs) dysfunction is associated with diabetes. We showed that oxidative stress was elevated in CACs cultured from blood of individuals with metabolic syndrome (MetS) and diabetes. We then assessed the action of palmitic acid (PA), a deregulated and increased NEFA in metabolic disorders, focusing on its oxidant potential. We observed that the phyto-polyphenol resveratrol normalized oxidative stress both in CACs isolated from MetS patients or treated with PA. Resveratrol further decreased the deleterious action of PA on gene expression of vascularization factors (TNF- α , VEGF-A, SDF-1 α , PECAM-1, VEGFR-2, Tie2 and CXCR4) and improved CAC motility. Particularly, resveratrol abolished the PA-induced overexpression of the pro-oxidant protein p66Shc. Neither KLF2 nor SIRT1, previously shown in resveratrol and p66Shc action, were directly involved. Silencing p66Shc normalized PA action on VEGF-A and TNF- α specifically, without abolishing the PA-induced oxidative stress, which suggests a deleterious role of p66Shc independently of any major modulation of the cellular oxidative status in a high NEFA levels context. Besides showing that resveratrol reverses PA-induced harmful effects on human CAC function, certainly through profound cellular modifications, we establish p66Shc as a major therapeutic target in metabolic disorders, independent from glycemic control.

1. INTRODUCTION

Circulating angiogenic cells (CACs), previously assimilated to early endothelial progenitor cells (EPCs), can be designated as angiogenic monocytes carrying progenitor features as differentiated *in vitro* from bone marrow-derived blood cells. These cells, which constitute approximately 3-6% of all circulating mononuclear cells can only be identified by culturing them *in vitro* for several days under endothelial growth conditions. They share hematopoietic, monocytic features such as endothelial markers after *in vitro* conditioning and resemble M2-like macrophages¹⁻³. They participate in revascularization entering the perivascular space of new blood vessels to improve their formation by secreting pro-vascularizing factors⁴. This process of neovascularization is strongly disturbed in diabetes. Depending on the type of pro-angiogenic cells, a defect in number, migration, adhesion or proliferation have been evidenced in patients and mouse models of diabetes, most of these dysfunctions being attributed to hyperglycemia^{5,6}.

Apart from high glucose, a growing body of evidence pointed out elevated plasma free fatty acids (FFA) levels as another harmful component of metabolic disorders and is considered as clinical manifestation of poor metabolic control in diabetic patients^{7,8}. Among saturated FFA, palmitic acid (PA), a 16-carbon non-esterified fatty acid (NEFA), is the most commonly encountered in western diet (30% of plasma NEFA) being present in meat, milk and palm oil⁹. Besides promoting endothelial oxidative stress¹⁰, PA dose and time-dependently affects function of myeloid¹¹ and non-myeloid EPC¹²⁻¹⁴ and hematopoietic progenitor cells¹⁴.

Recently, the small pro-oxidant protein p66Shc has been shown to be responsible for the hyperglycemia-induced reactive oxygen species (ROS) production in endothelial cells and mouse bone marrow-derived EPC *in vitro*, either contributing to the endothelial dysfunction or the altered angiogenic properties of streptozotocin hyperglycemic mice¹⁵⁻¹⁷. Furthermore, elevated mRNA levels of p66Shc were evidenced in monocytes isolated from diabetic patients compared to healthy controls¹⁸. Although the mechanisms of action of p66Shc are not clearly elucidated, it plays an important role as a mediator in intracellular signaling and seems to mainly act as a redox protein in mitochondria, contributing to the production of H_2O_2 ¹⁹.

Recent studies in endothelial cells have shown that the overexpression of a member of the sirtuin family, SIRT1, a major mammalian nicotinamide adenine dinucleotide-dependent deacetylase protein, prevents the high glucose-induced p66Shc upregulation, resulting in the abolition of hyperglycemia-induced dysfunction¹⁵. Likewise, the transcription factor Kruppel-like factor 2 (KLF2), a positive regulator of eNOS expression and anti-oxidant enzymes^{20,21}, has been negatively correlated with p66Shc expression in endothelial cells²². The pleiotropic beneficial action of the grape and red wine polyphenol compound resveratrol has been ascribed to its anti-oxidant and anti-inflammatory properties in multiple cell types including non-myeloid endothelial colony-forming cells (ECFC)²³. It can affect cell metabolism,

possibly through SIRT1 activation^{24,25}, although this remains controversial. Interestingly, part of the effects of resveratrol acts through KLF2 overexpression²⁶ as a downstream effect of the positive regulation of SIRT1. The numerous beneficial actions on metabolic and cardiovascular diseases²⁷ make this polyphenol a putative regulator of p66Shc.

In the present study, we thus studied the relation between NEFA and p66shc and ROS. We evaluated the beneficial action of resveratrol pre-treatment in healthy CACs submitted to pro-diabetic conditions such as high levels of PA and extended it to CACs isolated from patients therapeutic compound in metabolic diseases, underlining a modest effect in humans compared to animal studies and contrasting dose-effects²⁸, we showed here a clear beneficial action of resveratrol in improving CAC function in conditions of metabolic disorders.

2. MATERIALS AND METHODS

2.1. Patient characteristics

Peripheral blood samples were collected from male type 2 diabetic patients (T2DM) (n=20), individuals with the metabolic syndrome (MetS) (n=10) and healthy volunteers (n=10), after obtaining written informed consent. The study was approved by the institutional ethics board and conformed to the principles outlined in the Declaration of Helsinki.

2.2. CAC isolation and culture

CACs were differentiated from circulating mononuclear cells (MNCs) and their culture was assayed as described previously to isolate early EPC²⁹. In brief, MNCs were isolated by density gradient centrifugation with Ficoll separating solution (density 1.077) from human peripheral blood buffy coats or full blood. After several washing steps, 8×10^6 MNCs/ml of medium were plated on culture dishes coated with human fibronectin (Sigma) and maintained in endothelial basal medium (EBM; Cambrex, East Rutherford, NJ, USA) supplemented with EGM SingleQuots (Cambrex) and 20% fetal bovine serum (FBS). After 3 days in culture, non-adherent cells were removed by thorough washing with phosphate-buffered saline and fresh EGM was added until replacing 24 h before in vitro treatment with PA (200 μ M and 400 μ M) or high glucose (HG, 25 mM). Pre-treatment with resveratrol (30 μ M) was initiated 3 days before PA treatment. SIRT1 activator SRT1720 (4 μ M) or its vehicle DmsO were added on day 3 or day 6, 30 minutes before PA treatment. At day 7, adherent cells were stained with 2.4 μ g/ml DiI-Ac-LDL (Harbor Bio-Products, Norwood, MA, USA) at 37°C for 1 h and 10 μ g/ml FITC-Ulex europaeus lectin (Sigma-Aldrich). CACs are characterized as KDR⁺/Tie2⁺/CD31⁺/CD105⁺/CD34⁻/CD45⁺/CD14⁺/CD16⁺/CD68⁺/CD206⁻/CD163⁺ cells (data supplement Figure I).

2.3. Palmitic Acid preparation and treatment

Palmitic Acid (PA) (Sigma-Aldrich) solution was prepared as previously described³⁰. A conjugation of PA to BSA was prepared after PA was dissolved in 100% ethanol at 200 mmol/L and then combined with 10% FFA-free BSA in EBM to a concentration of 2 and 4 mmol/L. The stock solutions were adjusted to a pH of 7.4, filter sterilized and stored at -20°C. Vehicle control solution containing ethanol and BSA without PA was similarly prepared. The stock solutions were diluted daily at 1:10 directly in the cell culture medium (replaced 24 h before) for a 24 h treatment.

2.4. Lentivirus production for p66Shc silencing

Lentiviral shRNA constructs were obtained from the Sigma Mission library (Sigma-Aldrich St. Louis, MI). The human p66Shc-specific construct used was: TRCN0000009868 targeting the specific SHC1 isoform 1 and 3. The SHC002 non-target shRNA construct (Sigma-Aldrich) was used as a negative control. All shRNA construct were in the pLKO.1 vector backbone. shRNA-expressing lentiviral particles were prepared by transfection of HEK293T cells with pLKO.1 shRNA plasmid, together with the pMDL/pRRE, pVSV-G and pRSV-REV packaging plasmids, using the CalPhos Mammalian transfection kit (Clontech, Palo Alto, CA). Virus-containing medium was collected after 48 h post-transfection. Cultured CACs were infected with virus at day 3 post-isolation and medium was refreshed 24 h after the addition of virus. P66Shc silencing was determined by real time PCR and Western-blot.

2.5. Gene expression: Q-PCR analysis

Total RNA was isolated using RNeasy mini kit (Qiagen) according to the manufacturer's instructions. 200 to 500 ng of total RNA was reverse transcribed into cDNA using RevertAid H Minus First Strand cDNA Synthesis Kit (Fermentas, St. Leon-Rot, Germany) to assess the mRNA expression levels by real-time reverse transcriptase-polymerase chain reaction (RT-PCR). cDNA was then cleaned up with Minelute reaction cleanup kit (Qiagen) according to manufacturer's instructions. PCR reactions were performed in 10 µl volumes using Fast SYBR Green Master Mix (Applied Biosystems, Bleiswijk, The Netherlands) on an 7900HT Fast real-time PCR system (Applied Biosystems). Specificity of the amplification was checked by melt curve analysis. mRNA expression levels were corrected for expression of GAPDH and displayed as relative expression values. The following primer sequences were used in this study:

p66Shc	forward 5'-AAGTACAATCCACTCCGGAATGA-3'
	reverse 5'-GGGCCCCAGGGATGAAG-3'
VEGF-A	forward 5'-AGCACATAGGAGAGATGAGCTTC-3'
	reverse 5'-TGCTCTATCTTTCTTTGGTCTGCA-3'

VEGF-B	forward 5'-AGAGCTCAACCCAGACACCTG-3' reverse 5'-TCTGAAAAGCCATGTGTCACC-3'
SDF-1 α	forward 5'-TGCCCTTCAGATTGTAGCCC-3' reverse 5'-CAATGCACACTTGTCTGTTGTTGT-3'
TNFA	forward 5'-CCAAGCCCTGGTATGAGCC-3' reverse 5'-GCCGATTGATCTCAGCGC-3'
Angpt2	forward 5'-GATGGCAGCGTTGATTTTCA-3' reverse 5'-TCCCAGCCAATATTCTCCTGA-3'
PECAM-1	forward 5'-CTGATGCCGTGGAAAGCAG-3' reverse 5'-GCATCTGGCCTTGCTGTCTAA-3'
VEGFR-2	forward 5'-CCATCTTTTGGTGAATGGTG-3' reverse 5'-AGATGCCACAGACTCCCTGC-3'
CXCR4	forward 5'-AACCAGCGTTACCATGGAG-3' reverse 5'-CCATTTCCTCGGTGTAGTTATCTG-3'
KLF2	forward 5'-TTCTCGCGCTCCGATCAC-3' reverse 5'-CGGCTACATGTGCCGTTTC-3'
SIRT1	forward 5'-TCCTGGACAATTCCAGCCATCT-3' reverse 5'-ATCCTTTGGATTCCCGCAACCT-3'
GAPDH	forward 5'-GCCAGCCGAGCCACATC-3' reverse 5'-TGACCAGGCGCCCAATAC-3'

2.6. Western-blot analysis

For western blot analysis protein samples were denatured by boiling in sample buffer in the presence of 1% (w/v) SDS and separated by 7.5% SDS-PAGE. After electrophoresis, proteins were transferred to nitrocellulose membranes. Membranes were blocked for 1.5 hours with Odyssey Blocking Buffer (Li-Cor, Biosciences, Linclon, AK, USA) diluted 1:1 with phosphate buffered saline (PBS). Subsequently, Tween-20 was added to 0.1% (v/v) and incubation was continued overnight at 4°C in the presence of primary antibodies. The rabbit polyclonal anti-SHC1 antibody which recognizes a specific p66Shc N-terminal peptide (Abcam, ab103134) was used at 1/100 and incubated together with a mouse anti- α tubulin antibody (Cedarlane, Hornby, Ontario, Canada) diluted at 1/2000. After incubating with primary antibodies, the membranes were washed three times with PBS containing 0.1% Tween 20 (PBST). Then the membranes were incubated for 1 hour with IRDye800CW-conjugated goat anti-rabbit IgG and IRDye680-conjugated goat anti-mouse IgG secondary antibodies (LI-COR Biosciences) in Odyssey Blocking Buffer diluted 1:1 with PBS, 0.1% Tween-20. The blots were then washed three times with PBST and rinsed with PBS. Proteins were visualized by scanning the membrane on an Odyssey Infrared Imaging System (LI-COR Biosciences) with both 700- and 800-nm channels.

2.7. Conventional flow cytometry and Imaging flow cytometry analysis

Flow cytometry analysis was performed on CACs detached with 1 mM EDTA, washed with PBS 0.5% BSA and incubated for 45 min at room temperature with APC- and PE-labeled antibodies against KDR (VEGFR-2) (Biolegend) and CD309 (Tie2) (Milteny) and at 4°C with APC-labeled antibodies against CD105, CD16 (Immunotools), c-Kit (Biolegend), or PE-labeled antibodies against CD31 (PECAM-1) (Immunotools), CXCR4 (Biolegend), CD68 (eBioscience) and FITC-labeled antibodies against CD14 (Immunotools), CD34 (Macs Miltenyi Biotec). Antibodies against CD163 (Abd Serotec) and CD206 (BD Pharmingen) were revealed with a secondary goat anti-mouse alexa 488 antibody (Life Technologies). Cells were then washed and surface expression was quantified using a FACS calibur (BD Biosciences). As for imaging flow cytometry, cells were acquired on the ImageStreamX (Amnis corp.) imaging flow cytometer. Cells were acquired at 40x magnification and on the basis of their area (area = the number of pixels in an image reported in square microns). Minimum area for acquisition was set to 50 pixels. A minimum of 8000 cells was acquired per sample at a flow rate ranging between 50 and 100 cells/s. At least 2000 cells were acquired from single stained samples in order to allow for spectral compensation. Compensation samples were acquired with all channels habilitated and with the brightfield illumination and the 785 nm laser switched off. A minimum of 5000 cells from the single stained samples were acquired with the same settings as experimental samples in order to control for over/under compensation. Analysis was performed using the IDEAS v5.0 software (Amnis corp.). A compensation table was generated using the compensation macro built in the software. Single stained samples were manually gated for accurate calculation of spectral overlap coefficients. Once the compensation table was calculated for each of the staining sets, it was applied to the single staining samples that were acquired using the same settings as experimental samples. Proper compensation was then verified by visualizing samples in bivariate fluorescence intensity plots (data not shown).

2.8. Oxidative stress measurement

Cytoplasmic ROS production, hydrogen peroxide (H_2O_2) in particular, was evaluated after incubating the cells with 2 μ M 2',7'-chloromethyl-dichlorofluorescein-diacetate (CM-DCFH-DA, Invitrogen) at 37°C for 30 min. Once the acetate group is cleaved in the cytosol, the CM-DCFH non-fluorescent form of the probe is oxidized by intracellular H_2O_2 into CM-DCF fluorescent derivate. After washing out the probe and replacing the medium at room temperature, pictures of 5 random fields were immediately taken for each condition with an inverted fluorescence microscope in order to reveal CM-DCF green fluorescence. After applying a threshold for high fluorescence (ImageJ), CM-DCF-positive cells were counted. As for cells isolated from patients, they were seeded and stained in fibronectin-coated 8 well-chambers together with healthy controls. Pictures were taken with a widefield deconvolution

microscope and post-treatment image analysis was performed using the same conditions on healthy control and patient cells. The sum intensity of fluorescence was measured and normalized to the number of cells (Slidebook 4 software).

2.9. Chemotaxis and chemokinesis assay

CAC migration was performed using a Transwell Chamber (Corning Costar) for chemotaxis assay. Briefly, CACs were detached with 1 mM EDTA and resuspended in chemotaxis medium (1% BSA EBM). 100 μ l of cell suspension containing 2.10^4 cells were seeded in the upper compartment of a 2-chamber transwell divided by a membrane with 8 μ m pores coated with fibronectin. 600 μ l of chemotaxis medium alone or containing either 50 ng/ml VEGF, 100ng/ml SDF-1 α or the combination of VEGF and SDF-1 α were added to the lower compartment. After incubation at 37°C for 15 h, the upper chamber was removed and the membrane fixed in 4% PFA, free of extra medium. The non-migrated cells still present on the upper side of the membrane were wiped-out with a cotton stick. The remaining migrated cells were stained with Hoechst and counted on 5 fields per membrane under an inverted microscope. Chemokinesis function of CACs seeded on fibronectin coated 8 well-chambers in EGM was measured after analysis of videos recorded for 5 h using a live-cell inverted microscope. Chemokinetic migration capacity referred to the distance reached by CACs, following random movements, assessed using Image J software cell tracking.

2.10. Statistical analysis

Data were analyzed with Graphpad Prism 5 using paired Student's t-tests when comparing the effect of a treatment, or a one-way ANOVA with Bonferroni's correction for multiple comparisons. A non-parametric Kruskal-Wallis one-way ANOVA with Dunn's correction for multiple comparisons was performed to analyze oxidative stress data from patients. Probability values of $p < 0.05$ were considered significant and tests were performed two-sided. Data are presented as mean and error bars depict the standard error of the mean. n represents the number of blood donor.

3. RESULTS

3.1. CACs isolated from individuals with type 2 diabetes and the metabolic syndrome show increased oxidative stress, which is reversed by resveratrol

CACs were isolated and cultured for 7 days from blood obtained from T2DM patients and patients with metabolic syndrome (MetS), according to standard procedures. The baseline clinical characteristics of study participants are shown in Table 1.

Table 1: Patient characteristics

	Healthy n=10	MetS n=10	T2DM n=20
Age (years)	56 ±2	56 ±2	65 ±1**
BMI (kg/m ²)	28 ±1	31 ±1 #	29 ±1
HbA1C (%)	5.3 ±0.0	5.6 ±0.1	6.9 ±0.2**
Fasting glucose (mmol/L)	5.2 ±0.1	5.5 ±0.1	7.9 ±0.4**
Total cholesterol (mmol/L)	5.2 ±0.2	5.3 ±0.30	4.4 ±0.2
HDL cholesterol (mmol/L)	1.50 ±0.09	1.35 ±0.09	1.16 ±0.07 #
LDL cholesterol (mmol/L)	3.3 ±0.2	3.3 ±0.2	2.5 ±0.2
Fasting triglycerides (mmol/L)	1.0 ±0.1	1.5 ±0.2	1.6 ±0.2
NEFA (mmol/L)	0.36 ±0.02	0.40 ±0.10	0.47 ±0.02 #
Medication			
Metformin			100%
Statins		20%	76%
Anti-hypertensive drugs		40%	76%

** p≤0.01 vs. Healthy volunteers and MetS patients. # p≤0.05 vs. Healthy volunteers.

Despite a trend towards fewer cells isolated from diabetic patients, CAC number did not differ significantly from healthy controls (Figure 1A). However, T2DM and MetS CACs significantly displayed increased levels of H₂O₂ cytoplasmic production compared to healthy controls, as monitored by the oxidative sensitive fluorescent probe CM-DCFH-DA (Figure 1B). These increased oxidative levels were detected after a one-week culture, suggesting a prolonged, imprinted effect of the metabolic disorders but attenuated by resveratrol pre-treatment in T2DM CACs (Figure 1C). Resveratrol dose-dependently modulated oxidative stress in MetS CACs as 1 µM resveratrol did not affect the increase in H₂O₂ production in MetS cells (fold increase compared to healthy cells: non-treated vs. 1 µM resveratrol: 4.44 ±0.55 vs. 5.02 ±2.63; n=3) while 30 µM resveratrol completely reversed oxidative stress in MetS subjects.

3.2. High palmitic acid levels markedly increases p66Shc compared to high glucose

Oxidative stress was increased in CACs from diabetic patients, as indicated by the higher ROS production, but the accompanying apparent increase in p66Shc mRNA expression did not reach statistical significance compared to controls (Figure 2A). The impact of pro-diabetic conditions was then assessed in CACs isolated from healthy individuals. In contrast to former studies on HUVECs^{15,31}, we could not observe any significant rise of p66Shc mRNA expression after a 24 h-treatment with HG (25 mM) in CACs compared to its osmotic control mannitol (Figure 2B). However, while a 24 h-treatment with moderate concentrations of PA (200 µM) did not affect p66Shc gene expression, high levels of PA (400 µM) significantly increases p66Shc mRNA levels up to 5 fold compared to vehicle (Figure 2C). Interestingly, PA

200 μM only slightly increased these levels. PA 400 μM also substantially increased p66Shc protein expression (Figure 2D). In parallel, PA dose-dependently increased the inflammatory cytokine TNF- α , known to be upregulated in diabetes (Figure 2E). Conversely to published papers with near toxic levels of glucose, we observed that high levels of PA do not affect CAC number (Figure 2F).

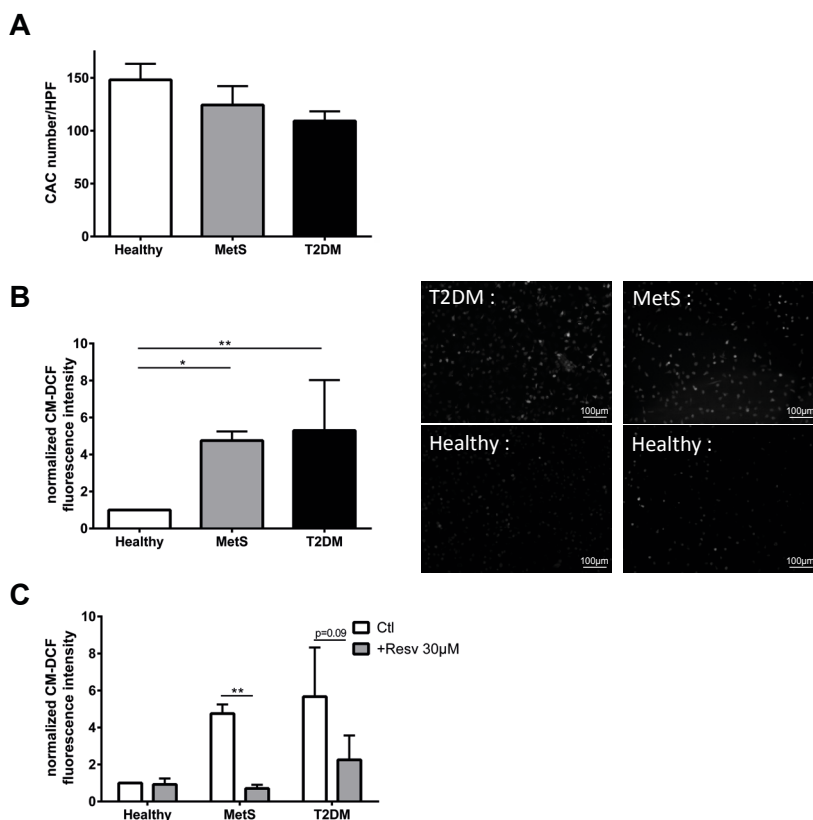


Figure 1: CACs isolated from of T2DM patients, MetS patients and healthy controls **A:** Number of CACs double positive for UEA Lectin and Dil-LDL uptake (n=10-12). **B and C:** Representative images of CACs incubated for 30 minutes with CM-DCFH-DA and visualized by fluorescent microscopy showing higher CM-DCF fluorescence intensity when isolated from MetS patients, compared to healthy cells visualized under identical imaging conditions. Resveratrol pre-treatment (Resv, 30 μM) reversed oxidative stress in CACs isolated from MetS patients (**C**). Bar graphs represent cellular CM-DCF fluorescence intensity normalized to healthy control CACs (n=3-4). *p<0.05; **p<0.01

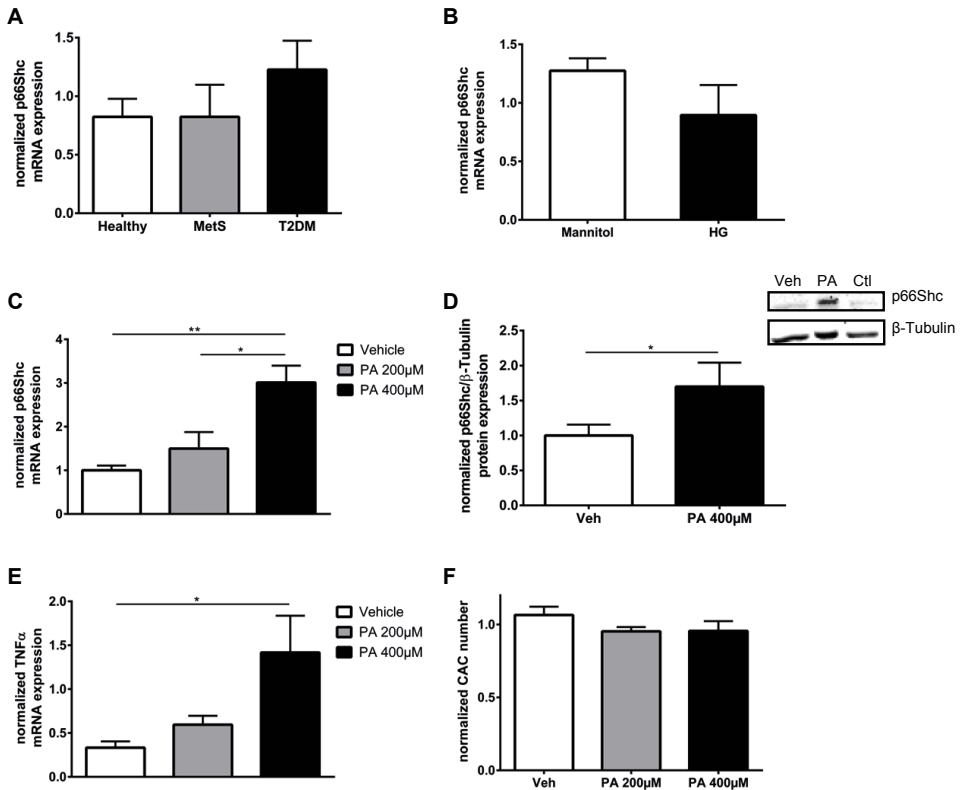


Figure 2: p66Shc expression in CACs: effect of 24 h-pro-diabetic conditions. **A:** Relative mRNA expression levels of p66Shc in CACs isolated from T2DM, MetS patients and healthy controls (**A**); in CACs treated with high glucose (HG, 25 mM) or the osmotic control Mannitol ($n=4$) (**B**) and with Palmitic Acid (PA) at 200 μ M, 400 μ M or the vehicle (Veh) control ($n=6-12$) (**C**). **D:** Representative western blot and quantitative analysis of p66Shc protein expression in CACs treated with PA 400 μ M or vehicle. Densitometric analysis of p66Shc and β -tubulin protein ratio is normalized to Veh ($n=7$). **E:** Relative mRNA expression levels of TNF- α in CACs treated with PA or Veh ($n=8$). **F:** Number of PA or Veh-treated CACs ($n=6$). Data are normalized to non-treated control cells, unless mentioned. * $p<0.05$; ** $p<0.01$

3.3. Effect of high palmitic acid levels on pro-vascularization factors

We further investigated PA impact on pro-vascularizing characteristics of CACs. PA action on gene expression (Figure 3A) underlines a downregulation of mRNA expression of the pro-vascularizing chemokine SDF-1 α without any major action on angiopoietin 2 (Angpt2). Conversely, PA 400 μ M induces a large rise in mRNA levels of the major pro-angiogenic cytokine VEGF-A, without affecting VEGF-B. In parallel, PECAM-1 was significantly affected by PA while no major action was observed on VEGFR-2 and CXCR4 mRNA levels. Nevertheless, imaging flow cytometry and classical FACS analysis (Figure 3B-C), showed that PA altered the surface expression of these important markers, highlighted here by the main decrease in fluorescent intensity observed on representative images of PA-treated cells stained for KDR (VEGFR-2) and Tie2 following flow cytometer imaging analysis.

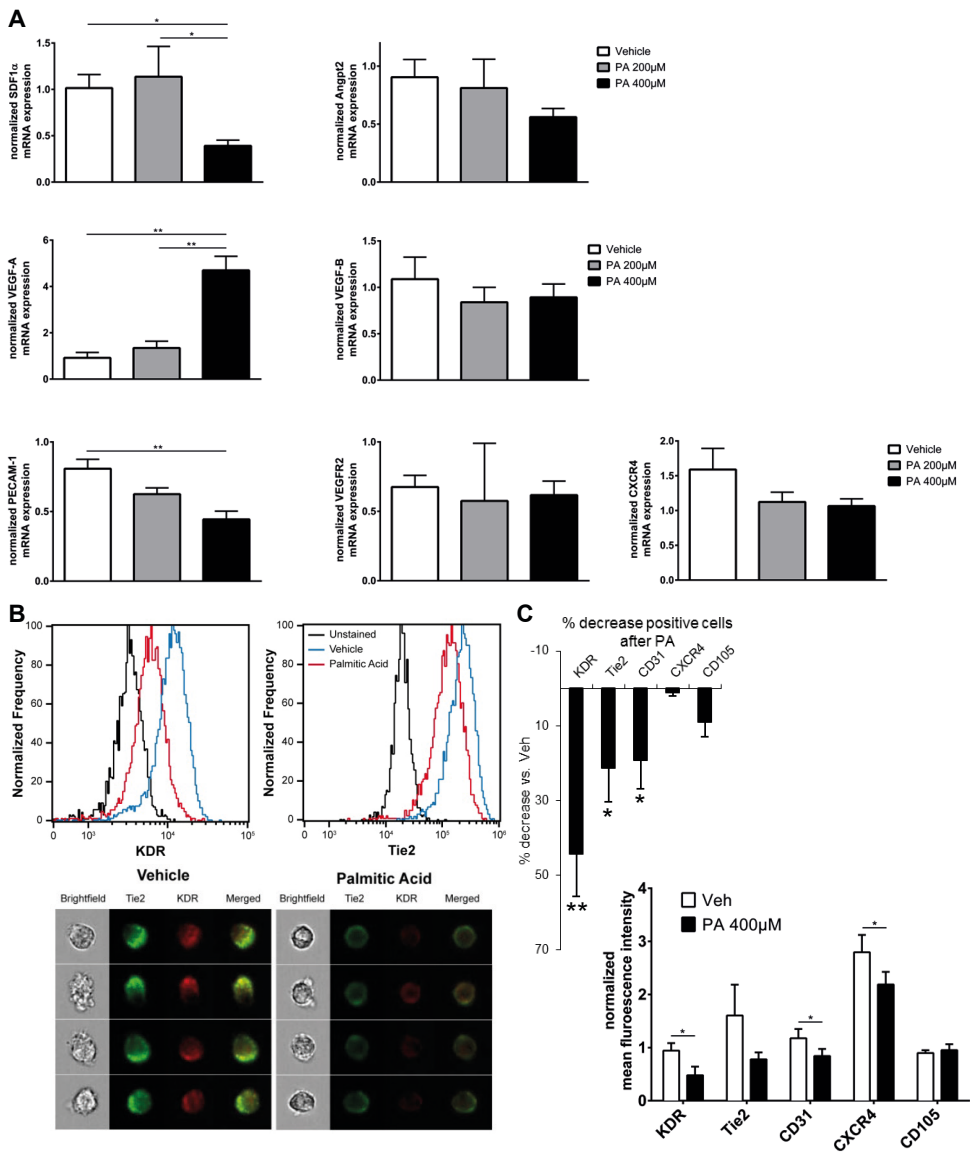


Figure 3: Effect of PA treatment on vascularization factors. **A:** Relative mRNA expression levels of vascularization cytokines or markers in CACs treated for 24 h with PA 200 μ M, 400 μ M or with vehicle (Veh) ($n=5-10$). **B:** Representative pictures of image flow cytometry of PA 400 μ M or vehicle-treated CACs and stained for KDR and Tie2 after Imagestream analysis and their associated mean fluorescence intensity (MFI) distribution histogram. **C:** Flow cytometry analysis of PA 400 μ M or vehicle-treated CACs and stained for indicated surface markers. Bar graphs represent the percentage of decrease in the number of positive cells treated with PA 400 μ M compared to vehicle-treated CACs (**left**). Surface expression expressed as MFI of PA 400 μ M or vehicle-treated CACs ($n=4-7$) (**right**). Data are normalized to non-treated control. * $p<0.05$; ** $p<0.01$

It resulted in a 60% drop in the number of KDR positive cells and, in a lesser extent, for PECAM-1 (CD31) and Tie2, after PA compared to vehicle. Although the number of CXCR4 positive cells was not affected, PA significantly decreased mean fluorescence intensity compared to vehicle. Of note, surface expression of progenitor markers such as endoglin (CD105) was only slightly attenuated.

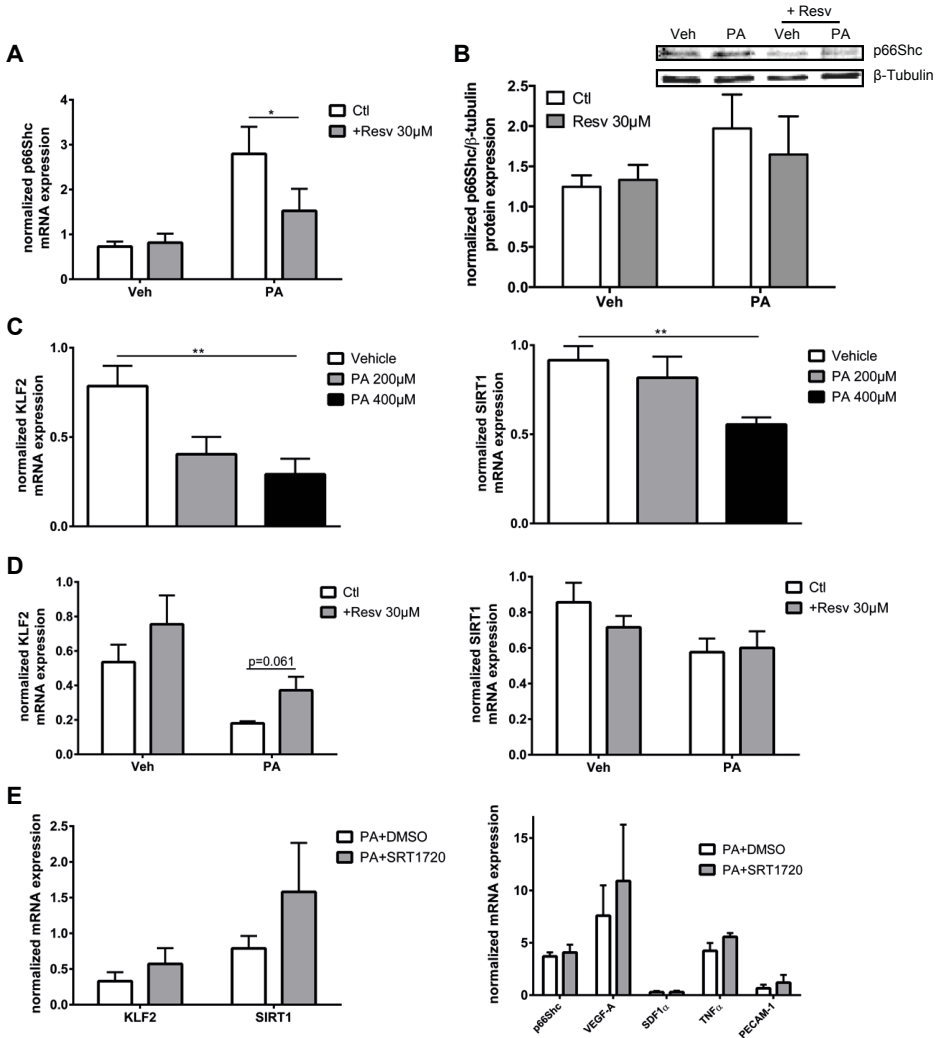


Figure 4: Resveratrol action on PA-induced p66Shc expression does not involve KLF2 and SIRT1. A and B: Effect of a pre-treatment with resveratrol (Resv, 30 μM for 3 days) on p66Shc mRNA (A) and protein expression quantification and representative western-blot (B) in PA 400 μM or vehicle (Veh)-treated CACs normalized to non-pre-treated control and vehicle (n=5-6). PA effect on relative mRNA expression levels of KLF2 and SIRT1 normalized to non-pre-treated control in CACs without (C) and with a pre-treatment with Resv (D) (n=5-10). **E:** Effect of a pre-treatment with the SIRT1 activator SRT1720 (4 μM, 30 minutes), or its vehicle DmsO, on relative mRNA expression levels of PA-treated CACs (n=4) normalized to Veh. *p<0.05; **p<0.01

3.4. Resveratrol prevents PA-induced p66Shc - role of KLF2 and SIRT1 activation

We next studied the action of resveratrol on PA-induced p66Shc expression in CACs. Figure 4A first shows that pre-treatment of CACs for 3 days with resveratrol before a 24 h-treatment with PA 400 μ M, normalized p66Shc levels by significantly decreasing PA action on p66Shc mRNA expression. At the protein level, resveratrol pre-treatment only limited p66Shc protein induction after PA treatment (Figure 4B).

We secondly assessed a putative modulation of KLF2 and SIRT1, known regulators of p66Shc in endothelial cells and putative actors of resveratrol effect. PA significantly affected gene expression of both KLF2 and SIRT1 in a dose-dependent manner (Figure 4C). However, whereas resveratrol has been described to upregulate KLF2 and SIRT1 mRNA expressions²⁶, no major changes could be observed after PA in CACs pre-treated with resveratrol (Figure 4D). Although KLF2 action is mainly regulated by its gene expression levels, SIRT1 activity is largely modulated post-transcriptionally. We thus aimed to mimic resveratrol action by using a SIRT1 activator (SRT1720; 4 μ M) (Figure 4E). We first noticed that SRT1720 pre-treatment for 3 days did not change p66Shc protein levels after PA treatment (Data supplement, Figure II). However, we observed that acute SIRT1 activation after shorter SRT1720 pre-treatment, which have been described before^{24,32}, tended to counteract PA-induced SIRT1 gene expression downregulation but did not affect PA-induced p66Shc mRNA upregulation nor impacted PA-mediated changes in the other gene expressions measured.

3.5. PA downstream effects do not involve p66Shc-induced oxidative stress nor TNF- α overexpression

We thus wondered if resveratrol could modulate the oxidative status of CACs, involving the regulation of the pro-oxidant protein p66Shc. To that end, oxidative stress was evaluated by the number of CM-DCF positive CACs. We first observed that a 24 h-PA treatment significantly increased oxidative stress in CACs (Figure 5A). Interestingly, pre-treatment with resveratrol markedly decreased the oxidative status of both PA and vehicle-treated CACs (Figure 5B). We hypothesized that the upregulation of the pro-oxidant protein p66Shc was directly responsible for the pro-oxidative action of PA. Unexpectedly, silencing p66Shc gene and protein expression (Data supplement, Figure III) did not alter the PA-induced increase in oxidative stress (Figure 5C), suggesting that ROS generated by PA do not involve p66Shc upregulation. Rather, knocking-down p66Shc directly affected the PA-induced changes in mRNA levels of VEGF-A and TNF- α in particular (Figure 5D). Furthermore, although an anti-oxidant treatment (NAC 5 mM) was previously shown to be effective on PA action³³, in our conditions, ROS scavenging did not prevent PA effect on gene expression levels (Figure 5E). We then speculated that the modulation of the inflammatory cytokine TNF- α by p66Shc would directly target VEGF-A expression. However, resveratrol only tended to prevent PA

action on the increase in TNF- α mRNA levels, suggesting its weak role in resveratrol effect (Figure 5F). Furthermore, CACs treated with TNF- α (10 ng/ml) for 24 h did not show any significant modulation of p66Shc, VEGF-A and SDF-1 α (Data supplement, Figure IV).

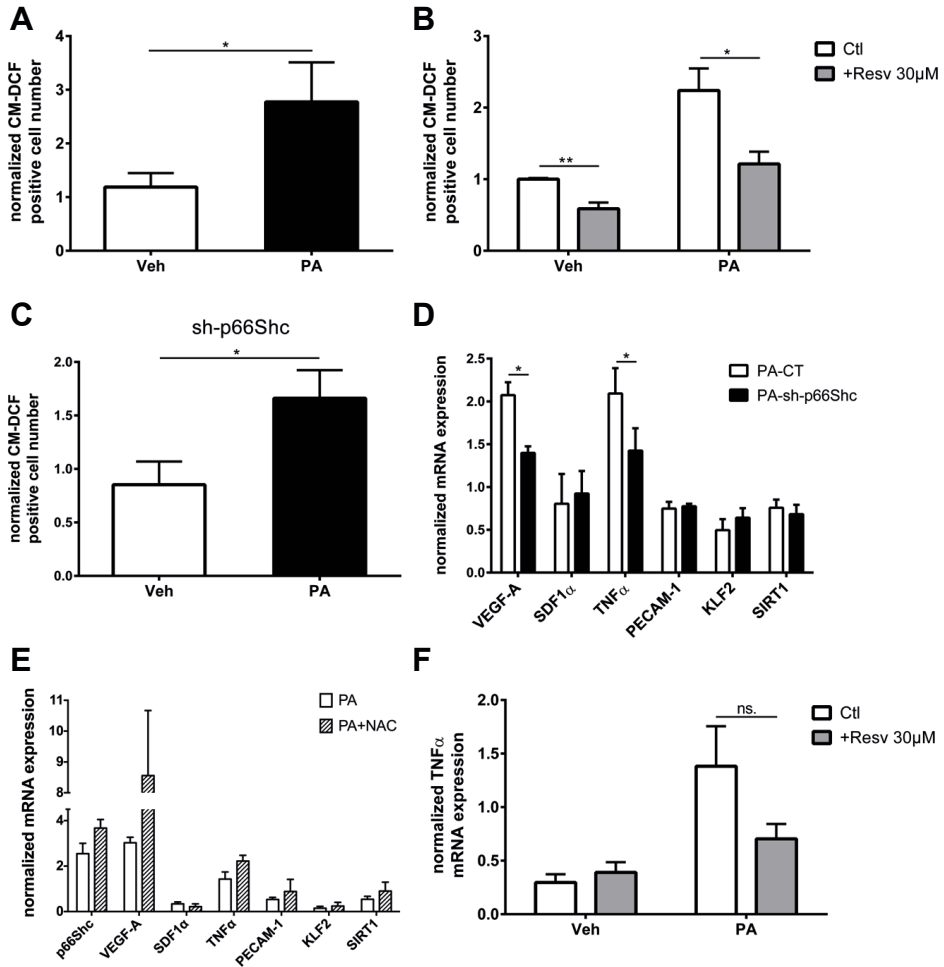


Figure 5: PA induces oxidative stress independently of p66Shc. **A and B:** PA-treated CACs visualized by fluorescent microscopy show higher number of CM-DCF positive cells compared to vehicle (Veh) normalized to control (**A**) (n=4). Resveratrol pre-treatment (Resv, 30 μ M) decreased oxidative stress in CACs treated with PA 400 μ M and Veh normalized to non-pretreated Veh (**B**) (n=5). **C and D:** Effects of p66Shc silencing in CACs submitted to lentiviral transduction with either a control non-target (CT) or with a p66Shc-targeted (sh-p66Shc) shRNA construct are normalized to vehicle-treated CT CACs (CT-Veh). PA-induced oxidative stress is not altered after p66Shc silencing (**C**) (n=4). Effect of p66Shc on relative mRNA expression levels of indicated genes (n=4) (**D**). **E:** Effect of a pre-treatment with an anti-oxidant (NAC 5 mM, 1 h) on gene expression after PA normalized to non-treated control (n=3). **F:** TNF- α mRNA expression is normalized to non-treated control (n=5). *p<0.05; **p<0.01; ns.: non significant

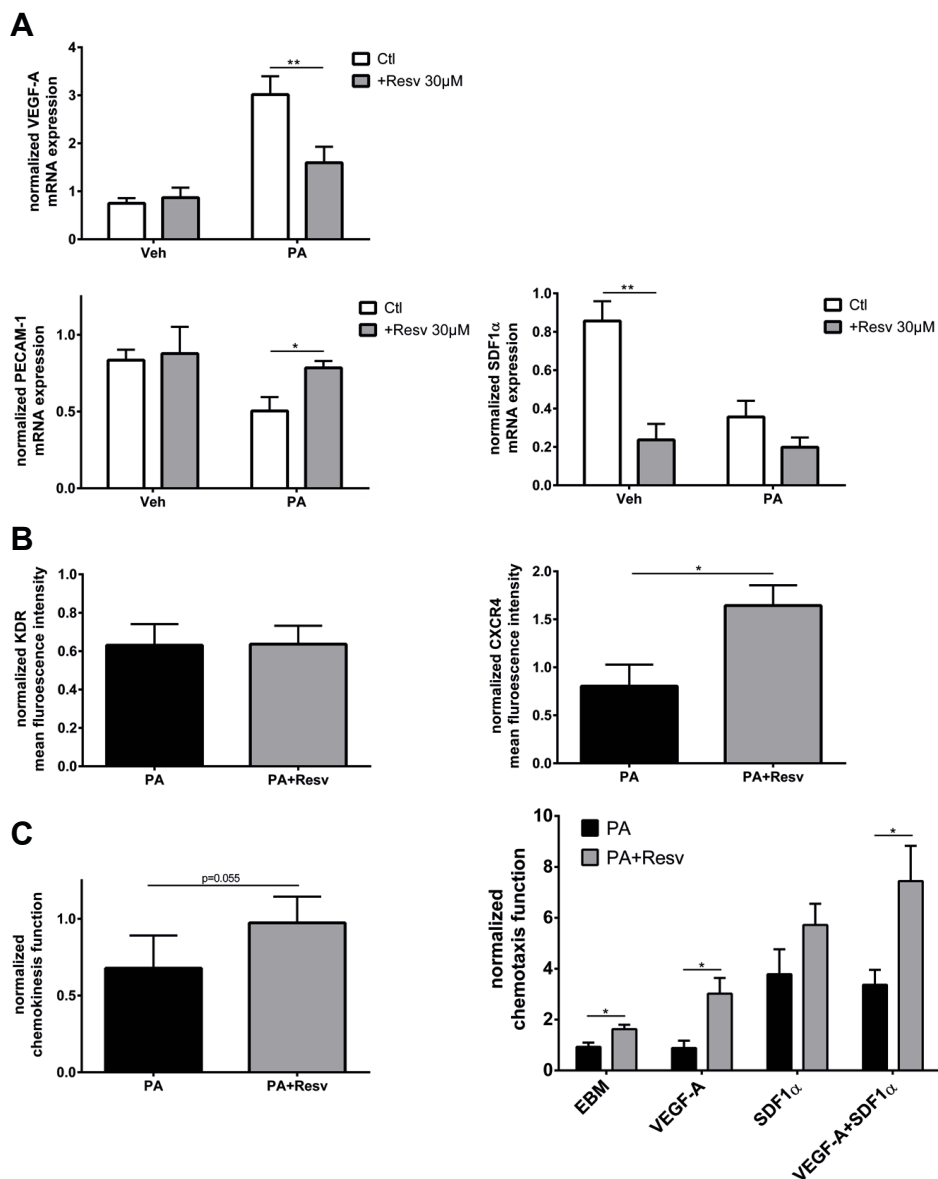


Figure 6: Resveratrol prevents downstream effects of PA to improve CAC function. **A:** Effect of a pre-treatment with resveratrol (Resv, 30 μM) on relative mRNA expression levels normalized to non-pre-treated control, in PA 400 μM or vehicle (Veh)-treated CACs compared to control conditions without pre-treatment (Ctl), (n=5-6). **B:** Flow cytometry analysis of CACs pre-treated or not with resveratrol before PA 400 μM and stained for KDR and CXCR4. Bar graphs represent mean fluorescent intensity normalized to Veh (n=3-4). **C:** Functional effects of resveratrol on CACs treated with PA 400 μM normalized to Veh. Chemokinesis function represents random cell movements in 5 hours (n=3) (**left**). Chemotaxis function refers to the number of migrated cells towards indicated chemokine agent (n=4) (**right**). *p<0.05; **p<0.01

3.6. Resveratrol prevents downstream effects of PA to improve CAC function

We finally assessed whether resveratrol had an action on the p66Shc-dependent downstream effects of PA. Resveratrol prevented the upregulation of VEGF-A mRNA levels and normalized the p66Shc-independent PECAM-1 gene expression after PA (Figure 6A). While completely abolishing the action of PA on SDF-1 α , resveratrol pre-treatment decreased mRNA levels in vehicle-treated cells. Considering the strong relationship of SDF-1 α expression with cellular oxidative status, the major anti-oxidant action of a 3-day resveratrol treatment could explain this specific gene downregulation. Conversely, resveratrol significantly increased CXCR4 surface expression in PA-treated CACs while it did not affect KDR intensity. Functional impact of these changes is shown on Figure 6B. Resveratrol pre-treatment tended to increase basic cell movements after PA in complete EGM and significantly stimulated chemokinesis in absence of any chemokine (in EBM + 1% BSA) using a chemotaxis assay (Figure 6C). Resveratrol significantly improved CAC migration towards VEGF-A but did not markedly towards SDF-1 α alone. Nevertheless, in the presence of both chemoattractants, migration of PA-treated CACs was increased by 2-fold after resveratrol, suggesting a particular beneficial action of resveratrol on the VEGF-A activation pathway.

4. DISCUSSION

Metabolic disorders, in particular type 2 diabetes, are linked to impaired EPCs but other pro-angiogenic cell types are also affected. P66Shc-induced oxidative stress is currently pointed out as a strong actor and mediator of deleterious consequences of diabetes. However, insights into the role of metabolic abnormalities other than hyperglycemia, such as elevated levels of circulating NEFA, have been poorly studied in this context. The major findings of this study showed that high levels of PA affected vascularization characteristics of CACs, which was in part a consequence of the marked upregulation of the pro-oxidant protein p66Shc, independently of their modified cellular oxidative status. In parallel, we unveiled a novel finding regarding to the action of resveratrol on angiogenic mononuclear cells, not yet tested to our knowledge. Indeed, resveratrol prevented PA effects and normalized oxidative stress in CACs isolated from patients with metabolic disorders.

One of our major findings is that PA modulates expression of different vascularization factors in a concentration dependent manner. Although a pro-inflammatory phenotype was described on PA-treated macrophages³⁴ to our knowledge, this is the first study showing that PA at a high concentration (400 μ M), which corresponds to NEFA plasmatic concentrations measured in diabetic patients in our study (Table 1) and others^{4,8} but not moderate levels (200 μ M), affects CAC pro-vascularizing characteristics without directly modifying viability, in contrast to what has been shown on late EPC¹²⁻¹⁴. High levels of PA decrease either gene and/or surface expressions of PECAM-1, CXCR4 and SDF-1 α , which may

have major deleterious consequences *in vivo*, reducing CAC extravasation and recruitment of further pro-angiogenic cells through SDF-1 α release at the sites of injury. Furthermore, PA counterintuitively increases VEGF-A gene expression, without affecting VEGF-B, which shows a selective regulation of the VEGF-A pro-angiogenic gene. Interestingly, we observed a decreased surface expression of different markers known to play a role in vascularizing action of CACs, such as VEGFR-2, Tie2 and CXCR4, without any changes in gene expression. A counter-regulation secondary to an excess of VEGF-A could explain the strongest PA effect seen on VEGFR-2 surface expression, as VEGF-A increases VEGFR-2 internalization and degradation³⁵. A strong upregulation of IL-8 mRNA expression seen under high PA conditions (data not shown) could also further over-activate VEGFR-2², leading to an unresponsive state characterized by a VEGFR-2 over-phosphorylation previously assessed in diabetic monocytes³⁶. Interestingly, VEGF-A signaling represents the major functional target of resveratrol in our study. In addition to normalize gene expression, resveratrol significantly increases the migration capacity of CACs without modulating VEGFR-2 surface expression altered by PA, most likely by increasing its functional sensitivity. As for CXCR4, its surface expression under PA is sufficient to maintain CAC migration capacity towards the SDF-1 α . As a consequence, CXCR4 induction by resveratrol may not add to the chemotactic capacity of CACs which may have reached a plateau as already observed before³⁷. Resveratrol improved chemokinesis in our study, a function previously shown to be controlled by NO production in CACs³⁷, which fits with a beneficial action shown on MNC-derived pro-angiogenic progenitor function *in vitro* and *in vivo* in a rat model of reendothelialization³⁸, accounting for an upregulation of eNOS. In our model, we could not observe any alteration of eNOS mRNA levels (data not shown) after PA, but we cannot exclude that resveratrol could improve NO bioavailability by modulating PA-induced oxidative stress and participate in the known benefits of NO on CAC function^{37,39}.

Among resveratrol downstream targets, the pro-oxidant protein p66shc could be a putative candidate. We observed for the first time that in normoglycemic conditions, PA induced p66Shc overexpression in CACs. Despite conflicting reports, we did not observe any action of high glucose on p66Shc expression in CACs although the majority of studies were conducted in endothelial cells. Nevertheless, Di Stefano *et al* observed an abolition of the pro-oxidant action of prolonged hyperglycemia *in vitro*, in p66Shc-deficient bone marrow-derived early EPCs¹⁷. Conversely, in our PA-induced oxidative stress conditions, directly and solely silencing p66Shc did not affect the increased ROS production, which was shown to be directly linked to ceramide elevation after PA⁴⁰. However, an important finding is that p66Shc mediates PA action on gene expression of important factors modulating vascularization VEGF-A and TNF- α without affecting the oxidative status of CACs. The normalization of VEGF-A mRNA expression after resveratrol in PA-treated CACs could then be caused, in part, by the associated decrease in p66Shc expression.

The regulation of p66Shc gene expression was shown to be controlled by SIRT1 in hyperglycemic endothelial cells¹⁵. In contrast to resveratrol pre-treatment, the direct SIRT1 activator SRT1720 had no action on p66Shc expression, excluding the hypothesis of a sole SIRT1 modulation playing a role in PA action. Resveratrol neither markedly modulated PA-induced KLF2 downregulation suggesting that the normalization of p66Shc expression does not directly involve KLF2 levels. To summarize, neither SIRT1 activation nor KLF2 upregulation seem to be directly involved in PA-induced p66Shc overexpression, however we cannot exclude their additive role in the resveratrol-mediated normalization of PA action. We hypothesized that resveratrol could attenuate oxidative stress and p66Shc expression in part through the modulation of TNF- α . Such as in macrophages³⁴, PA induces TNF- α expression; however neither TNF- α alone nor an anti-oxidant treatment added prior to PA significantly modulated gene expressions and p66Shc, VEGF-A and SDF-1 α in particular. The regulation of p66Shc gene transcription is highly regulated epigenetically either by p53⁴¹ or through promoter hypermethylation by homocysteine⁴². We cannot exclude similar mechanisms happening in CACs, as high NEFA modulates p53 in monocytes⁷.

In our conditions, although the survival of CACs isolated from MetS or T2DM is not affected, as previously observed before³⁹, an interesting novel observation underlined an increased oxidative stress in this specific cell type compared to aged-matched healthy cells, even after 7 days of *in vitro* culture. This finding is of major importance as it evidences and transposes to CACs the principle of harmful metabolic memory already attributed to hyperglycemia or HbA1C, once cells were placed in normal conditions. The concept of metabolic memory was shown to have clinical relevance by several large-sized outcome trials in T2DM. Indeed, recent hyperglycemia mega-trials showed that aggressive blood glucose lowering in patients with long-standing T2DM, who had poor glycemic control for years and had developed cardiovascular damage, had no beneficial effects on cardiovascular outcome, suggesting an irreversible impact of previously uncontrolled glycemia on the vasculature⁴³.

Most interestingly, a role of p66Shc was recently evidenced in the process of endothelial hyperglycemic memory³¹. Thus, after normalization of the cellular environment following elevated NEFA conditions, p66Shc upregulation might play a deleterious role in particular regarding to the regulation of important cytokines such as VEGF-A and TNF- α .

5. CONCLUSIONS

We showed for the first time that high levels of NEFA increase oxidative stress in angiogenic mononuclear cells in parallel to a p66Shc upregulation, which was completely reversed by resveratrol (Data supplement Figure V). We thus point out this compound as a putative therapeutic tool in the context of metabolic disorders and p66Shc-linked pathologies. Most interestingly, these data unexpectedly highlight a deleterious role of p66Shc besides any

major modulation of the cellular oxidative status in a high NEFA level context, establishing p66Shc as a major target for conjunctive therapy in metabolic disorders, independent from glycemic control.

Acknowledgements

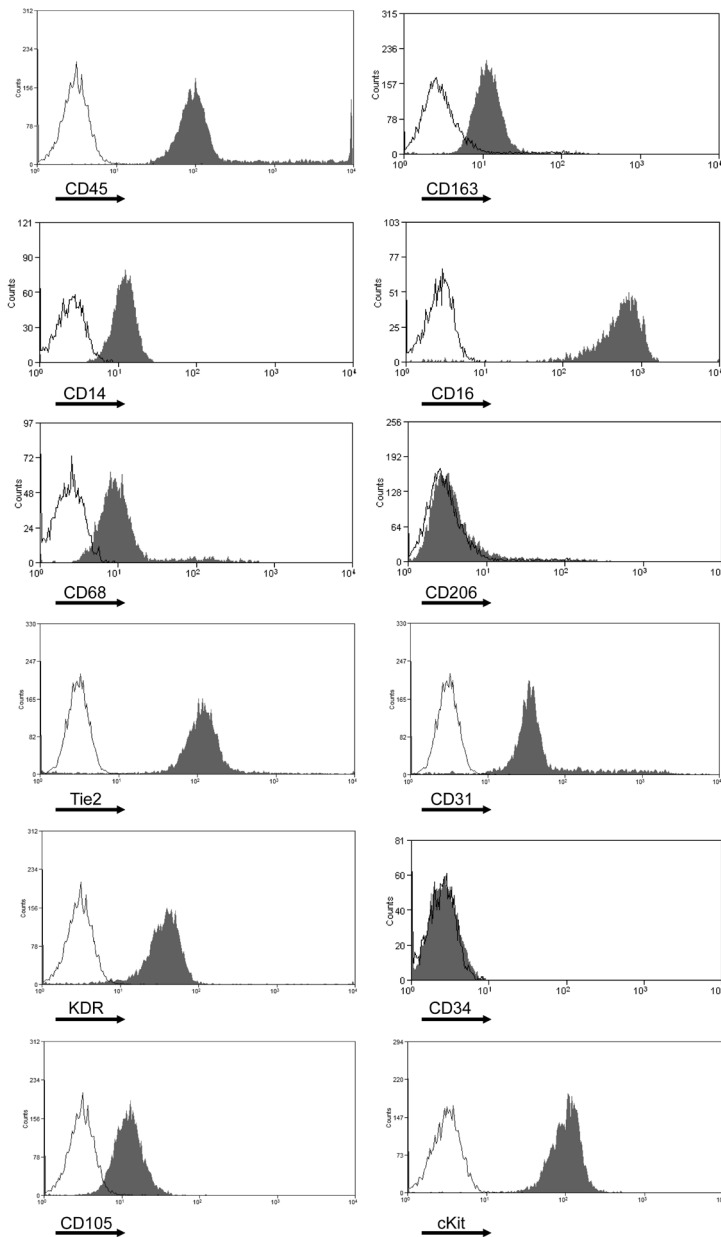
This work was supported by a European Marie Curie's IEF fellowship (FP7 254644 EPCrepair project). The content is solely the responsibility of the authors and does not necessarily represent the official views of the ERC. We thank Dr. Gilles Kauffenstein for his help in finalizing the manuscript.

REFERENCES

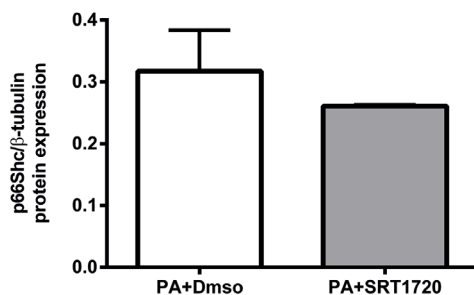
1. van der Pouw Kraan TC, van der Laan, A. M., Piek, J. J. & Horrevoets, A. J. Surfing the data tsunami, a bioinformatic dissection of the proangiogenic monocyte. *Vascul. Pharmacol.* 56, 297-305 (2012).
2. Medina, R. J. *et al.* Myeloid angiogenic cells act as alternative M2 macrophages and modulate angiogenesis through interleukin-8. *Mol. Med.* 17, 1045-1055 (2011).
3. Favre, J., Terborg, N. & Horrevoets, A. J. The diverse identity of angiogenic monocytes. *Eur. J. Clin. Invest.* 43, 100-107 (2013).
4. Urbich, C. & Dimmeler, S. Endothelial progenitor cells: characterization and role in vascular biology. *Circ. Res.* 95, 343-353 (2004).
5. Tepper, O. M. *et al.* Human endothelial progenitor cells from type II diabetics exhibit impaired proliferation, adhesion, and incorporation into vascular structures. *Circulation.* 106, 2781-2786 (2002).
6. Silvestre, J. S. Vascular progenitor cells and diabetes: role in postischemic neovascularisation. *Diabetes Metab.* 34 Suppl 1:S33-6. doi: 10.1016/S1262-3636,-0 (2008).
7. de Kreutzenberg, S. V. *et al.* Downregulation of the longevity-associated protein sirtuin 1 in insulin resistance and metabolic syndrome: potential biochemical mechanisms. *Diabetes.* 59, 1006-1015 (2010).
8. Karpe, F., Dickmann, J. R. & Frayn, K. N. Fatty acids, obesity, and insulin resistance: time for a reevaluation. *Diabetes.* 60, 2441-2449 (2011).
9. Stumvoll, M., Nurjhan, N., Perriello, G., Dailey, G. & Gerich, J. E. Metabolic effects of metformin in non-insulin-dependent diabetes mellitus. *N. Engl. J. Med.* 333, 550-554 (1995).
10. Inoguchi, T. *et al.* High glucose level and free fatty acid stimulate reactive oxygen species production through protein kinase C--dependent activation of NAD(P)H oxidase in cultured vascular cells. *Diabetes.* 49, 1939-1945 (2000).
11. Xia, L. *et al.* Resveratrol reduces endothelial progenitor cells senescence through augmentation of telomerase activity by Akt-dependent mechanisms. *Br. J. Pharmacol.* 155, 387-394 (2008).
12. Trombetta, A. *et al.* Increase of palmitic acid concentration impairs endothelial progenitor cell and bone marrow-derived progenitor cell bioavailability: role of the STAT5/PPARgamma transcriptional complex. *Diabetes.* 62, 1245-1257 (2013).
13. Guo, W. X. *et al.* Palmitic and linoleic acids impair endothelial progenitor cells by inhibition of Akt/eNOS pathway. *Arch. Med. Res.* 39, 434-442 (2008).
14. Jiang, H. *et al.* Palmitic acid promotes endothelial progenitor cells apoptosis via p38 and JNK mitogen-activated protein kinase pathways. *Atherosclerosis.* 210, 71-77 (2010).
15. Zhou, S. *et al.* Repression of P66Shc expression by SIRT1 contributes to the prevention of hyperglycemia-induced endothelial dysfunction. *Circ. Res.* 109, 639-648 (2011).
16. Camici, G. G. *et al.* Genetic deletion of p66(Shc) adaptor protein prevents hyperglycemia-induced endothelial dysfunction and oxidative stress. *Proc. Natl. Acad. Sci. U. S. A.* 104, 5217-5222 (2007).
17. Di, S., V *et al.* p66ShcA modulates oxidative stress and survival of endothelial progenitor cells in response to high glucose. *Cardiovasc. Res.* 82, 421-429 (2009).
18. Pagnin, E. *et al.* Diabetes induces p66shc gene expression in human peripheral blood mononuclear cells: relationship to oxidative stress. *J. Clin. Endocrinol. Metab.* 90, 1130-1136 (2005).
19. Giorgio, M. *et al.* Electron transfer between cytochrome c and p66Shc generates reactive oxygen species that trigger mitochondrial apoptosis. *Cell.* 122, 221-233 (2005).
20. van Thienen, J. V. *et al.* Shear stress sustains atheroprotective endothelial KLF2 expression more potently than statins through mRNA stabilization. *Cardiovasc. Res.* 72, 231-240 (2006).
21. Dekker, R. J. *et al.* KLF2 provokes a gene expression pattern that establishes functional quiescent differentiation of the endothelium. *Blood.* 107, 4354-4363 (2006).
22. Kumar, A. *et al.* Transcriptional repression of Kruppel like factor-2 by the adaptor protein p66shc. *FASEB J.* 23, 4344-4352 (2009).
23. Vassallo, P. F. *et al.* Accelerated senescence of cord blood endothelial progenitor cells in premature neonates is driven by SIRT1 decreased expression. *Blood.* 123, 2116-2126 (2014).
24. Milne, J. C. *et al.* Small molecule activators of SIRT1 as therapeutics for the treatment of type 2 diabetes. *Nature.* 450, 712-716 (2007).

25. Park, S. J. *et al.* Resveratrol ameliorates aging-related metabolic phenotypes by inhibiting cAMP phosphodiesterases. *Cell*. 148, 421-433 (2012).
26. Gracia-Sancho, J., Villarreal, G., Jr., Zhang, Y. & Garcia-Cardena, G. Activation of SIRT1 by resveratrol induces KLF2 expression conferring an endothelial vasoprotective phenotype. *Cardiovasc. Res.* 85, 514-519 (2010).
27. Chung, J. H., Manganiello, V. & Dyck, J. R. Resveratrol as a calorie restriction mimetic: therapeutic implications. *Trends Cell Biol.* 22, 546-554 (2012).
28. Pollack, R. M. & Crandall, J. P. Resveratrol: therapeutic potential for improving cardiometabolic health. *Am. J. Hypertens.* 26, 1260-1268 (2013).
29. Boon, R. A. *et al.* Kruppel-like factor 2 improves neovascularization capacity of aged proangiogenic cells. *Eur. Heart J.* 32, 371-377 (2011).
30. Wang, X. L. *et al.* Free fatty acids inhibit insulin signaling-stimulated endothelial nitric oxide synthase activation through upregulating PTEN or inhibiting Akt kinase. *Diabetes.* 55, 2301-2310 (2006).
31. Paneni, F. *et al.* Gene silencing of the mitochondrial adaptor p66(Shc) suppresses vascular hyperglycemic memory in diabetes. *Circ. Res.* %20;111, 278-289 (2012).
32. Jiang, S., Wang, W., Miner, J. & Fromm, M. Cross regulation of sirtuin 1, AMPK, and PPARgamma in conjugated linoleic acid treated adipocytes. *PLoS. One.* 7, e48874 (2012).
33. Yuzefovych, L., Wilson, G. & Rachev, L. Different effects of oleate vs. palmitate on mitochondrial function, apoptosis, and insulin signaling in L6 skeletal muscle cells: role of oxidative stress. *Am. J. Physiol Endocrinol. Metab.* 299, E1096-E1105 (2010).
34. Haversen, L., Danielsson, K. N., Fogelstrand, L. & Wiklund, O. Induction of proinflammatory cytokines by long-chain saturated fatty acids in human macrophages. *Atherosclerosis.* 202, 382-393 (2009).
35. Ewan, L. C. *et al.* Intrinsic tyrosine kinase activity is required for vascular endothelial growth factor receptor 2 ubiquitination, sorting and degradation in endothelial cells. *Traffic.* 7, 1270-1282 (2006).
36. Tchaikovski, V., Olieslagers, S., Bohmer, F. D. & Waltenberger, J. Diabetes mellitus activates signal transduction pathways resulting in vascular endothelial growth factor resistance of human monocytes. *Circulation.* 120, 150-159 (2009).
37. Heiss, C. *et al.* Nitric oxide synthase expression and functional response to nitric oxide are both important modulators of circulating angiogenic cell response to angiogenic stimuli. *Arterioscler. Thromb. Biol.* 30, 2212-2218 (2010).
38. J G *et al.* Effects of resveratrol on endothelial progenitor cells and their contributions to reendothelialization in intima-injured rats. *J. Cardiovasc. Pharmacol.* 47, 711-721 (2006).
39. Mangialardi, G. *et al.* Nitric oxide-donating statin improves multiple functions of circulating angiogenic cells. *Br. J. Pharmacol.* 164, 570-583 (2011).
40. Mehra, V. C. *et al.* Ceramide-activated phosphatase mediates fatty acid-induced endothelial VEGF resistance and impaired angiogenesis. *Am. J. Pathol.* 184, 1562-1576 (2014).
41. Kim, C. S. *et al.* p53 impairs endothelium-dependent vasomotor function through transcriptional upregulation of p66shc. *Circ. Res.* 103, 1441-1450 (2008).
42. Kim, C. S. *et al.* Homocysteine promotes human endothelial cell dysfunction via site-specific epigenetic regulation of p66shc. *Cardiovasc. Res.* 92, 466-475 (2011).
43. Giacco, F. & Brownlee, M. Oxidative stress and diabetic complications. *Circ. Res.* 107, 1058-1070 (2010).

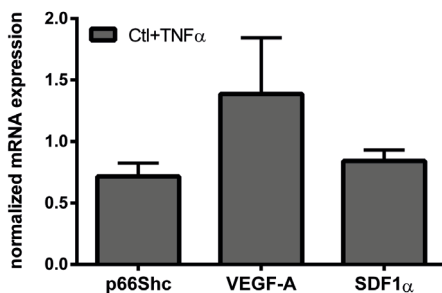
SUPPLEMENTARY INFORMATION



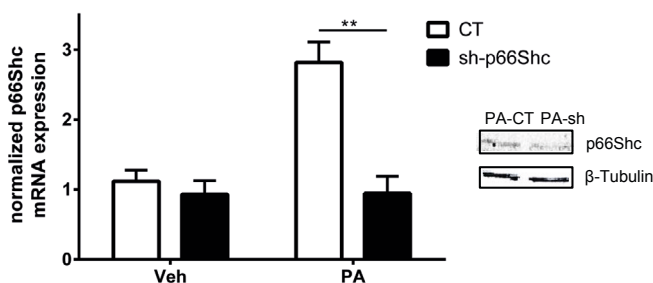
Supplement Figure I: Characterization of CACs by flow cytometry. Representative histograms of mean fluorescence intensity of unstained CACs (open) and CACs stained for indicated markers after FACS analysis, showing characteristics of hematopoietic, monocyte, macrophage, endothelial and progenitor surface markers.



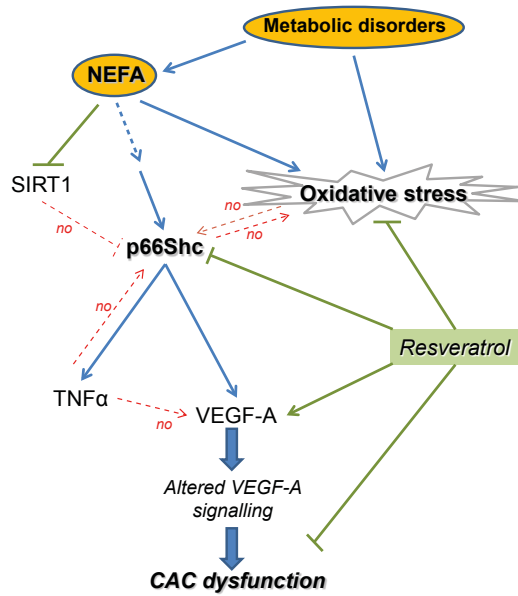
Supplement Figure II: SIRT1 activator does not modify p66Shc expression. Western blot analysis of p66Shc protein expression of PA (400 μ M)-treated CACs submitted or not to a pre-treatment with the SIRT1 activator SRT1720 (4 μ M for 3 days), or its vehicle Dms0. Densitometric analysis of p66Shc protein expression was normalized on β -tubulin (n=3).



Supplement Figure III: TNF- α does not modify expression of PA-downstream gene targets. Effect of a 24 h-treatment control CACs with TNF- α (10 ng/ml) at day 6 post-isolation on relative mRNA expression level. Bar graphs represent fold changes with respect to non-treated control CACs (n=3).



Supplement Figure IV: p66Shc silencing. Efficiency of p66Shc silencing in CACs submitted to lentiviral transduction with either a control non-target (CT) or with a p66Shc-targeted (Sh-p66Shc) shRNA construct is evidenced under PA conditions. Bar graphs represent relative mRNA expression levels of p66Shc in CACs normalized to non-treated control (n=5). Representative western blot shows a parallel decrease in p66Shc protein expression. **p<0.01



Supplement Figure V: Schematic representation of the proposed mechanism of action of resveratrol in metabolic disorder conditions in CACs. High levels of PA increase p66Shc expression independently of SIRT1 downregulation. This p66Shc overexpression, independent of the cellular oxidative status, is responsible for the PA-induced TNF- α and VEGF-A upregulation but not for the increase in oxidative stress. In contrast, resveratrol pre-treatment blunts the elevated oxidative stress due to chronic metabolic disorders or acute PA treatment, in which condition it normalizes NEFA action on p66Shc and VEGF-A in particular, finally improving CAC function such as chemotaxis and chemokinesis. Red dashed lines represent hypothesis tested and excluded experimentally in our study.

